The mechanisms of aluminum-induced immunotoxicity in chicks

Changyu Cao,[*,†] Yaozu Liu,[*] Zhiqing Yang,[*] Huimin Ouyang,[*] Qiang Fu,[*,†] and Xinran Li[*,†,1]

[*]*College of Life Science and Engineering, Foshan University, Foshan, Guangdong, 528231, P. R. China; and* [†]*Foshan University Veterinary Teaching Hospital, Foshan, Guangdong 528231, P. R. China*

ABSTRACT Aluminum (**Al**) is a ubiquitous environmental pollutant representing a significant global health hazard to human and animal health, including chicks. Al toxicity causes oxidative stress, leading to tissue injury, and consequently causes various diseases. NRF2 signaling is vital for protecting cells against oxidative stress. Nuclear xenobiotic receptors are activated by exogenous toxins, thereby inducing the transcription of cytochrome P450 enzyme systems (**CYP450s)** isoforms involved in xenobiotic metabolism and transport. However, little is known about Al-induced oxidative stress, nuclear xenobiotic receptors and fibrosis in chicks and the mechanisms involved. In this study, male chicks were treated with 0 mg/kg and 500 mg/kg $Al_2(SO_4)_3$ to evaluate the mechanisms for Al-induced immunotoxicity. Histopathology revealed pathological injury, fibrin aggregation, disruption of the Nuclear Xenobiotic Receptors, and alteration of CYP450s homeostasis in Al-treated chicks due to oxidative stress. Notably, regulation of the NRF2 pathway and CYP450s and fibrosis-related genes was found to play a vital role in inhibiting immunotoxicity. This study provides new insights regarding the mechanisms of Al-induced immunotoxicity, including activation of the nuclear xenobiotic receptors, triggering oxidative stress, and altering the homeostasis of CYP450s in chicks. Further, it provides a theoretical basis for controlling Al exposure and highlights the importance of further studying its mechanisms to provide additional information for formulating preventive measures.

Key words: Aluminum, Immunotoxicity, Chick, Spleen and Bursa of Fabricius

2023 Poultry Science 102:102251
https://doi.org/10.1016/j.psj.2022.102251

INTRODUCTION

Aluminum (**Al**) is a ubiquitous pollutant, including biological materials. Food is the main source of exposure for humans and animals. Air-borne particulates, fumes, pharmaceuticals such as antacids, and vaccines with Al as an adjuvant are additional exposure sources for humans and animals. Studies demonstrate that Al^{3+} is mainly absorbed from the gastrointestinal tract and spreads throughout the body, consequently accumulating in different tissues (Riihimäki and Aitio, 2012). The spleen and bursa of fabricius are important immune organs in the body. They are rich in lymphocytes, macrophages, and erythrocytes and are the center of humoral and cellular immunity (Tarantino et al., 2011), playing a crucial role in maintaining immune homeostasis. Al can accumulate in the immune organs, leading to tissue injury, including structural damage and immunosuppression. Moreover, Al triggers oxidative damage, thereby impairing cellular signaling cascades by increasing the production of reactive oxygen and reactive nitrogen species (ROS and RNS), consequently leading to organ damage in the subsequent events.

The immune system is a potential target for $Al_2(SO_4)_3$. It causes toxicity in neurologic, hematopoietic, skeletal, respiratory, and immunologic systems (Willhite et al., 2012). It can also cause biochemical and metabolic disorders, inducing tissue damage because of oxidative damage, contributing to disease pathogenesis. Oxidative redox factors including SOD, MDA, and GSH are targets of Al attack. Furthermore, Al toxicity induces skin keratinization and granular parakeratosis (Fujii et al., 2020), damages synaptic plasticity, and impair rats' learning and memory functions (Qin et al., 2020). It also induces male reproductive damage through the apoptosis signaling pathway in animals (Güvenç et al., 2020) and tissue fibrosis (Contini et al., 2016; Igbokwe et al., 2019). Tissue fibrosis is highlighted by an inflammatory response and collagen deposition leading to organ failure. Tissue fibrosis is mainly regulated by the TGF-β1, TIMP-1, MMPs, and cytochrome P450 enzyme system (**CYP450**) genes (Wang et al., 2019).

Received January 4, 2022.
Accepted October 11, 2022.

[1]Corresponding author: lixinran@fosu.edu.cn

Despite the significant health concerns associated with Al toxicity, only a few in vivo studies highlight its oral and immunotoxicity. This research thus focused on Al-induced damage to the immune organs after acute Al poisoning to explain Al's toxicological mechanisms, including fibrosis and apoptosis. This study constitutes a useful model for predicting the potential immunotoxicity of Al in chicks (spleen and bursa of fabricius), useful for the assessment of the potential toxicity of Al in wildlife.

MATERIALS AND METHODS

Animals and Experimental Design

Seven-day-old immunized chicks were randomly divided into 2 groups (n = 20): an experimental and a control group. Chicks in the experimental group were administered 500 mg/kg Al sulfate through gavage, while those in the control group were administered with distilled water through gavage. The chicks were then subjected to fasting for 24 h, after which they were sacrificed, and their organs separated under ice bags. Their spleen and bursa of fabricius tissues were collected and stored at −80°C, awaiting analysis.

Histopathological Examination

Spleen and bursa of fabricius samples were rapidly fixed in 10% formaldehyde for 24 h and embedded in paraffin. They were then cut into 5-μm thick sections and stained with hematoxylin and eosin (**H&E**), and Masson trichrome and subsequently observed under a light microscope.

Measurement of Oxidative Stress Indices

The oxidative stress indices, including glutathione peroxidasetotal (**Gpx**), glutathione (**GSH**), antioxidant capacity (**T-AOC**), total super-oxide dismutase (**SOD**), catalase (**CAT**), hydrogen peroxide ($\mathbf{H_2O_2}$), and malondialdehyde (**MDA**) were determined in 10% tissue homogenates using detection kits (Nanjing Jiancheng bioengineering institute, Nanjing, China) following the manufacturer's instructions. The levels of Gpx, GSH, T-AOC, CAT, H_2O_2, and MDA were assayed using the colorimetric method at 412 nm, 420 nm, 520 nm, 405 nm, 405 nm, and 532 nm, respectively. The activity of SOD was assayed at 550 nm using the hydroxylamine method.

Quantitative Reverse Transcription-Polymerase Chain Reaction Analysis

Total RNA was extracted from the spleen and bursa of fabricius tissues, and the RevertAid first-strand cDNA synthesis kit was subsequently used to synthesize the RNA to cDNA. The Fast Universal SYBR Green Master Mix was then used to measure the gene expression levels on a Light Cycler 480 System. The genes included the NRF2 and its downstream genes, fibrosis related genes, GSTs isoforms, and CYP450 genes. A Primer Analysis Software (Oligo 7.0) was used to design target-specific oligonucleotide primers (Table 1), then commercially synthesized by the Beijing Genomics Institute Co., Ltd., China. The housekeeping genes, GAPDH and β-actin, were used as the internal reference. The relative abundance of the mRNA for each gene was normalized to the mean expression of GAPDH and β-actin and calculated using the $2^{-\Delta\Delta Ct}$ method. The mRNA abundance accounted for gene-specific efficiency.

Statistical Analysis

Data were analyzed using the GraphPad Prism 7.0 (GraphPad Software Inc., San Diego, CA), imageJ 1.8 (National Institutes of Health [**NIH**], Bethesda, MD) and SPSS 20 software and presented as means ± SD to determine the effects of the dietary FB1. Multiple comparisons of means were performed using a one-way analysis of variance (**ANOVA**). A P value <0.05 was set as the significance threshold.

RESULTS

Histopathological Analyses of Spleen and Bursa of Fabricius Tissues

No gross changes or significant changes in clinical features in the spleen or bursa of fabricus were found. The red and white pulp in the spleen of chicks in the control group were clear, with no obvious abnormalities in the splenic cord and sinus structure. However, the boundary between the red pulp and white pulp in chicks in the Al group was blurred, with a decrease in the number of spleen cells and cell shrinkage (Figure 1). In the same line, the bursa of fabricius of chicks in the control group had a complete structure, the medullary cortex had clear boundaries, and the cells were tightly arranged, with no cell debris and cavities. In contrast, chicks in the Al group had widened grassroots gaps, with a loss of the epithelial cell layer, cavities in the cortex and medulla, and a decrease in lymphocytes (Figure 1). These findings indicated that acute Al exposure damaged the cellular structure of the spleen and bursa of fabricius.

Detection of Oxidative Stress Markers of Spleen and Bursa of Fabricius

Al exposure induced the activities of Gpx, GSH, CAT, SOD, and MDA in the spleen and bursa of fabricius ($P < 0.05$). Notably, T-AOC activity decreased, while the level of H_2O_2 increased in Al treated bursa of fabricius ($P < 0.05$, Figure 2). These results suggested that the induction of oxidative stress was one of the mechanisms of Al-induced tissue damage.

Table 1. The Sequences of oligonucleotide primers.

Gene name	LOCUS	Upstream Primer sequence (5′-3′)	Downstream Primer sequence (5′-3′)	Size (bp)
COL1A2	NM_001079714.2	ACTTCATACCTAGCAACAAGCCA	AGCAAAATTTCCGCCAAGACC	183
COL2A1	NM_204426.2	CCGCGACCTCCGACAACCT	GTGCCGGGTTCTCCATCCCTT	189
COL4A1	NM_001162399.3	GCTGATTTACCATGGCTACTCCC	ACCAGTGATAGGTGCCATACTCA	220
COL5A1	NM_204790.4	CGACCTGGATAAAGACTTCACCG	GGCCTCCGATCCCTTCGTA	140
COL6A1	NM_205107.20	ATCCTGGTGCTTATGGACCCAA	TGTTGCCAGGAGCACCCTTC	111
COL6A2	NM_205348.4	AGGCTCTTCTCAGACCTCG	CACTGGGCTACTGCAAGCTC	122
COL6A3	NM_205534.3	CCTTGATATTGGCCGTGACA	GGCACTGACTAAATCGGCTT	112
MMP-1	XM_417176.6	ATATGACATTGTACGTGGCTA	CTGCACAGCATCATCAGAC	108
MMP-2	NM_204420.3	CGCCACTGAGATTTAACCGAA	GATAGCCATCACCATGTTCCC	84
MMP-3	XM_046909299.1	GTCAAAAGAACCTGTACTGCC	ATATGCAGCGTCAACACCA	193
MMP-7	NM_001006278.1	CTTCCGTTTCCAGTACCAC	TTCTGCATTTAATTTTCCGGTT	183
MMP-9	NM_204667.2	CAGCTACGACGCCGACAAGACC	GCACACCAGCGATAGCCGTCA	165
MMP-11	XM_004934502.4	CGATGTGACACCGCTGACCTT	CCAGGTTGTTCCCGATCGTCCA	203
MMP-13	AF070478.1	CCTCGAAAACTCAAATGGTCA	ACCATGTTCTTTAGTGCCAA	198
TIMP2	NM_204298.2	GCCCCGACCAGGACATCGAA	TGCCATCGCCCTCGGATTTGC	120
TIMP3	NM_205487.3	GTTCTGCAACTCCGACATCGT	CGGTCCCATTTCTCATACCAA	276
AHR	AF192502.2	ACAGCAGGAATTAGATCAGCA	GCTCCAATTTGTGAACATCCCA	133
CYP 1A1	NM_205147.2	AATGCTCGTTTCAGTGCCTT	TGCCCAATCAATGAGTCCGT	101
CYP 1A2	XM_046924517.1	CCGACTCCCTCATCGAGCAGT	AAGCCTGCTCCAAAGATGTCA	112
CYP 1A5	X99454.1	ACCGTTGCGTGTTTATCAACCAG	ACTTCGGTCCCTTCAGCGTT	109
CYP 1B1	XM_040668785.2	ACATGCAGTTTGAAAGTAAGCCT	TTCCAGAGATGCTCCAACCAG	100
CAR	NM_204702.2	CGCCTCCAGAAGTGCCTCGAC	TGTGCCTGCGCCAACCTCC	110
PXR	NM_205294.2	ATCCTTCTCCCATCGCTCT	CCCAGCTCCGACTTATCCAT	171
CYP 2C18	NM_001001752.3	AAAGAAGCCTTGATTGATCGT	CGTGTAACCATCCCTCGTTG	118
CYP 2C45	AJ430584.1	TAGTCTAGCATACTCGTGGCTT	AGATTTCTCGCTTTCATCAGG	218
CYP 2D6	NM_001195557.2	CTCACATGACATACCGGGACA	CAGGGTAAAATTCATTTGGCTT	129
CYP 3A4	XM_046927350.1	CCTTCCGTCCCAGATCACA	AAATTGCTGAGAAAAGTGCCT	170
CYP 3A7	NM_001001751.2	CCCCAGATCATCAAAACCG	TTCAGCTAATGAGACAGCGTT	108
NRF2	NM_205117.1	CTGCCCAAAACTGCCGTA	TCAAATCTTGCTCCAGTTCCA	60
HO-1	NM_205344.1	GCTGAAGAAAATCGCCCAA	ATCTCAAGGGCATTCATTCGG	135
SOD1	NM_205064.1	TGTGCATGAATTTGGAGACAAC	TTGCAGTCACATTGCCGAG	131
SOD2	NM_204211.1	TGCACTGAAATTCAATGGT	GTTTCTCCTTGAAGTTTGCG	146
SOD3	XM_420760.3	TTTTCTCCTAAAGATGGCAAG	CTTCCTGCTCATGGATCACAA	109
CAT	NM_001031215.2	CAAGTTCCACGTTAAGACCGAT	TAATCAGGATCAGTAGAAGCCAGT	84
GCLC	XM_015859246.1	TCTGTAGATGATCGAACGC	TCCTTTATTAGGTGCTCGTAG	176
GCLM	XM_015870028.1	GCTGCTAACTCACAATGACC	TGCATGATATAGCCTTTGGAC	174
NQO1	NM_205518.1	CTCCGAGTGCTTTGTCTACG	AATGGCTGGCATCTCAAACC	151
GSTA2	NM_001001776.1	GCCTGACTTCAGTCCTTGGT	CCACCGAATTGACTCCATCT	138
GSTA3	NM_001001777.1	GATGAACGTCGTCCAACCAG	TCATGTCCGTGGTCCTTCAA	117
GSTA4	XM_046913019.1	CTTTCTTGTGGGAAACCGAT	AGGAACTTCTTAATTGTAGGCAT	156
GSTM2	NM_205090.1	GACTTCCCCAACCTGCCCTA	CTGCTTCTCCACCTCCGTCT	120
GSTO1	XM_015867248.1	TCTGTAATTTCCAAGGCACT	GAGTCCCCACCATAAAACACA	128
GSTT1	XM_015878095.1	CTCTTCACAGGGCAACCAC	GATCTGCCAAGGAAATCTCG	139
GAPDH	NM_204305.1	AGAACATCATCCCAGCGT	AGCCTTCACTACCCTCTTG	182
β-actin	NM_205518.1	CTCTCGGCTGTGGTGGTGAA	CCGCTCTATGAAGGCTACGC	128

Induction of the NRF2 Signaling Pathways and GSTs Isoforms in the Spleen and Bursa of Fabricius by Al

There was an increase ($P < 0.05$) in the transcription level of the relative factors, including NRF2, HO-1, NQO-1, GSTO1, and GSTT1 of the NRF2 signaling pathways in spleen and bursa of fabricius in the Al group than in the control group. However, other factors, including SOD1, SOD2, SOD3, CAT, GCLM, GSTA2, GSTA3, and GSTA4, were restrained in the Al group than in the control group. We, thus hypothesized that Al induces tissue damage by regulating the transcription level of Nrf2 signaling pathways and GSTs isoforms genes (Figure 3).

Induction of Fibrosis of the Spleen and Bursa of Fabricius by Al

The fibrosis induced by FB1 was further evaluated through Masson trichrome staining (Figure 4A) and the expression of fibrosis-associated genes (Figure 4B). Masson staining is one of the staining methods used to detect collagen fibres in animal tissues. It dyes the collagen fibres blue and displays their content, thus revealing the degree of fibrosis. In this study, the collagen in the Al treated spleen and bursa of fabricius were distributed in a denser band than that of the control group. Al significantly upregulated the mRNA expressions of TIMP2, TIMP3, MMP-2, MMP-7, COL1A2, and COL2A1 in the spleen and bursa of fabricius. However, it decreased the mRNA expressions of MMP-9 in the spleen and bursa of fabricius, and COL4A1, COL5A1, and MMP3 in the spleen. These results revealed that Al exposure induces tissue fibrosis that is mediated by the MMP-TIMP-Collagen pathway.

Induction of CYP450 Homeostasis and Nuclear Xenobiotic Receptors Response Disorder in Spleen and Bursa of Fabricius by Al

CYP450 and the CYP450 subunit were detected to explore the effects of Al on CYP450 homeostasis

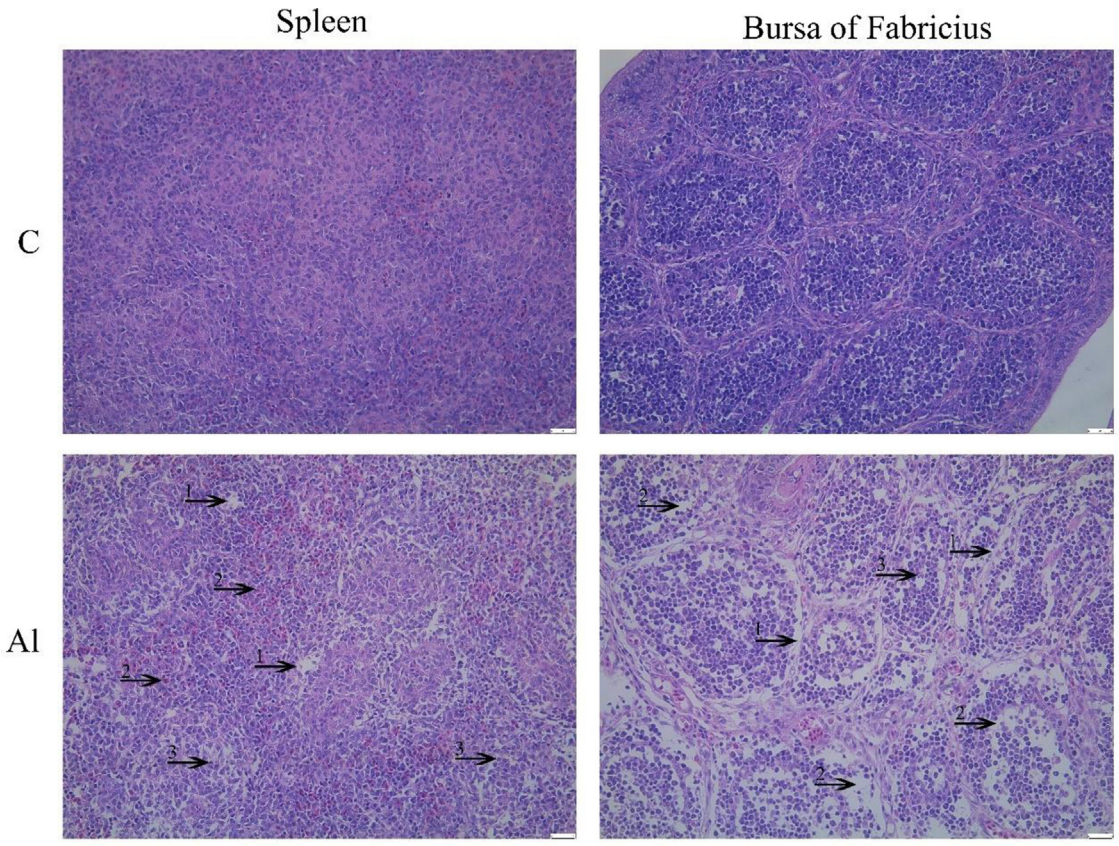

Figure 1. Effects of Al on the histopathology of chick spleen and bursa of fabricus (scale bar = 20 μm). In the spleen, **1** shows the hollow cells, **2** the Red pulp area, and **3** the lymphocytes. In the bursa of fabric, **1** shows the epithelial cell layer, **2** the cortex and medulla, and **3** the lymphocytes. **C** and **Al** represents the Control and Al group, respectively.

(Figure 5). The xenobiotic-sensing nuclear receptors (**NXRs**) response which regulates CYP450, was also determined by detecting the relative mRNA level of NXRs (AHR, CAR, and PXR) and its target genes using qRT-PCR. There was a decline in the CAR and PXR subunits (2C18, 2C45, 3A7, and 3A9) and an augment of the AHR subunit (1A4 and 1A5) in the Al group than in the control group ($P < 0.05$). These findings suggested that Al inhibited the transcription of NXRs and altered the homeostasis of CYP450 in the spleen and bursa of fabricius of chicks.

DISCUSSION

The spleen and bursa of fabricius are important immune organs in poultry. They are the major players in maintaining immune homeostasis. Previous studies postulate that Al can inhibit the body's innate immune function, causing immune toxicity in mice (Liu et al., 2020). To date, the published data on the oral immunotoxicity of acute Al poisoning are scarce. This study focused on the potential risks of acute Al toxicity in chick spleen and bursa of fabricus by investigating its

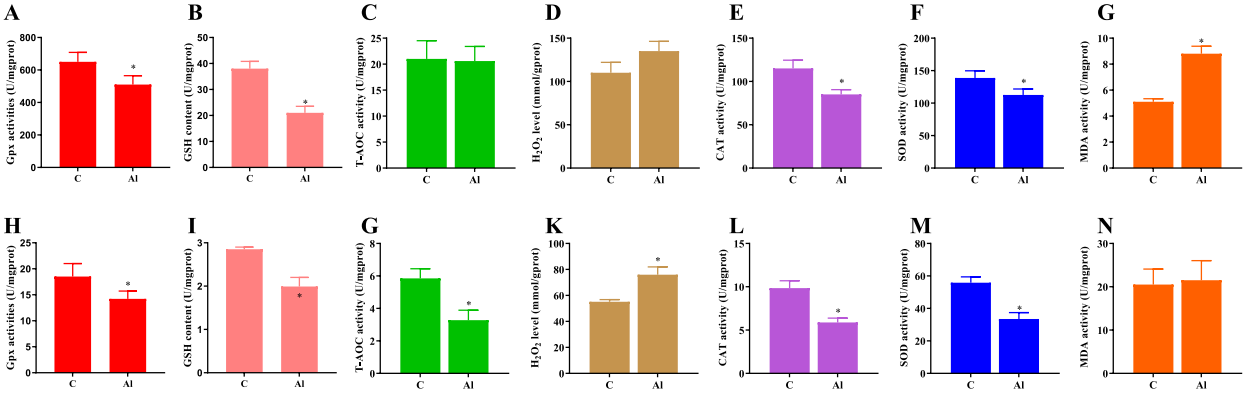

Figure 2. Al-induced oxidative stress in the spleen and bursa of fabricus of the chicks (n = 8 in each group). (A–G) Gpx activity, GSH content, T-AOC activity, H_2O_2 level, CAT activity, SOD activity, and MDA activity in spleen; (H–N) Gpx activity, GSH content, T-AOC activity, H_2O_2 level, CAT activity, SOD activity, and MDA activity in bursa of fabricus. Data are presented as the means ± SD. $^*P < 0.05$ denotes significant differences between the control group and Al group.

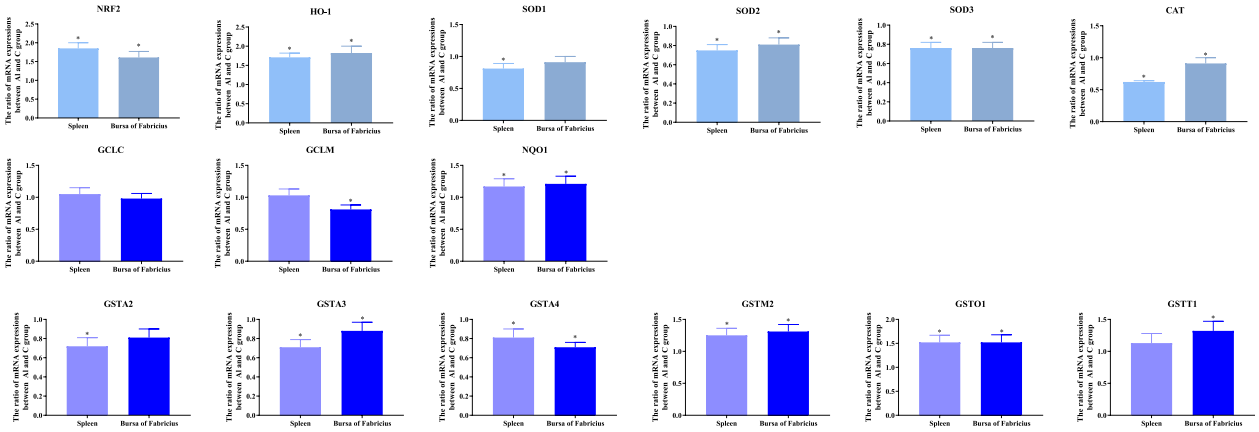

Figure 3. Bar graphs showing the effects of Al on the mRNA expression of NRF2 and its downstream genes in the spleen and bursa of fabricus.

effects on oxidative stress, CYP450 homeostasis, and fibrosis. This study demonstrated that acute Al toxicity was closely associated with oxidative stress and fibrosis, which led to tissue damage. Further, oxidative stress and fibrosis were mediated by the NRF2 pathways and regulated by CYP450s homeostasis. This study provided new evidence for the immunotoxicity of Al in chicks.

The immune system is the most sensitive body system to exogenous stimulation. The adverse effects of exogenous substances are primarily reflected in morphological changes of the immune organs. Spleen hemorrhage and bursa inflammatory cell infiltration caused by Al exposure fully reflected the toxic effect of Al. These toxic effects are generally irreversible and may cause cell death and tissue damage (Li et al., 2020).

Oxidative stress, characterized by the imbalance between oxidation and antioxidant systems, is one of the principal pathological mechanism of Al-induced immunotoxicity. SOD, CAT, and GSH are vital antioxidant indicators modulating oxidative injury. A decrease of Gpx, GSH, CAT, and SOD indicates a decreased ability to scavenge free radicals, leading to oxidative stress. In the same line, an increase of MDA reflects enhanced lipid peroxidation and tissue injury. The findings of this study were consistent with those of Cao et al. which reported elevated antioxidant enzyme SOD activity and GSH level in the hippocampus of Al-exposed rats (Cao et al., 2019). The findings strongly suggested the induction of oxidative stress as the mechanism underlying Al-induced immune organ lesions.

Antioxidant enzymes, including GSH, CAT, and SOD can be activated by NRF2 to prevent excessive oxidative damage, thus enhancing their activities as adaptive intracellular responses. NRF2 is an emerging regulator of oxidative stress. Its downregulation decreases the expression of the primary antioxidative enzyme. Al-induced downregulation of the expression of NRF2, thus, enhances detoxification (Zali and RezaeI, 2014). An assessment of the NRF2 downstream genes to confirm the activation of the signaling pathway revealed an increase in HO-1, NQO1, GSTO1, and GSTT1, and a decrease in the mRNA of SOD1, SOD2, SOD3, and CAT compared to the control group.

Nrf2 also regulates GSH synthesis enzymes such as NQO1, HO-1, and GST. NQO1 is a target for bioreductive activation of antioxidants and a mediator of xenobiotic detoxification. GCL catalyzes the rate-limiting step in the biosynthesis of GSH and combines with toxic components, thus accelerating Al excretion (Gong et al., 2015). Al led to elevated levels of NRF2, thus promoting the transcriptional induction of several Phase II detoxification genes, including GSTA and GSTM. This finding confirmed the critical role of NRF2 in reducing Al-induced toxicity (Park et al., 2019).

GST is an important protein that acts as a link between NRF2 and CYP450 (Bao et al., 2019). CYP450 expression assays were performed to evaluate whether NRF2 initiates downstream responses following oxidative stress. In this study, the homeostasis of the CYP450 enzyme system was altered, accompanied by the activation of NXR because of the severe oxidative stress caused by Al toxicity. Xenobiotic receptors, including the PXR, AHR, and CAR, play important roles in sensing foreign chemicals (xenobiotics) and triggering detoxification and metabolism pathways in different host tissues (Erickson et al., 2019). In this study, most of the mRNA expressions of CYP450 subunits decreased in Al treated chicks, attributed to the increased levels of oxidative stress and decreased levels of PXR, CAR, and AHR. Changes in these genes respond to tissue stress induced by acute Al poisoning. Al can enter the tissue and cells, interact with the NXRs, and elicit CYP disorders, thereby inducing cell damage and oxidative stress, which aggravates damage to the spleen and bursa of fabricius. In vivo studies postulate that exogenous toxins inhibit the AHR pathway in the kidneys of zebrafish and chicken while exhibiting tissue selectivity and specificity (Chen and Chan, 2018; Q. Zhang et al., 2020). The findings of this study collectively suggest that acute Al poison activates the NXR response in chicks. However, additional studies will be

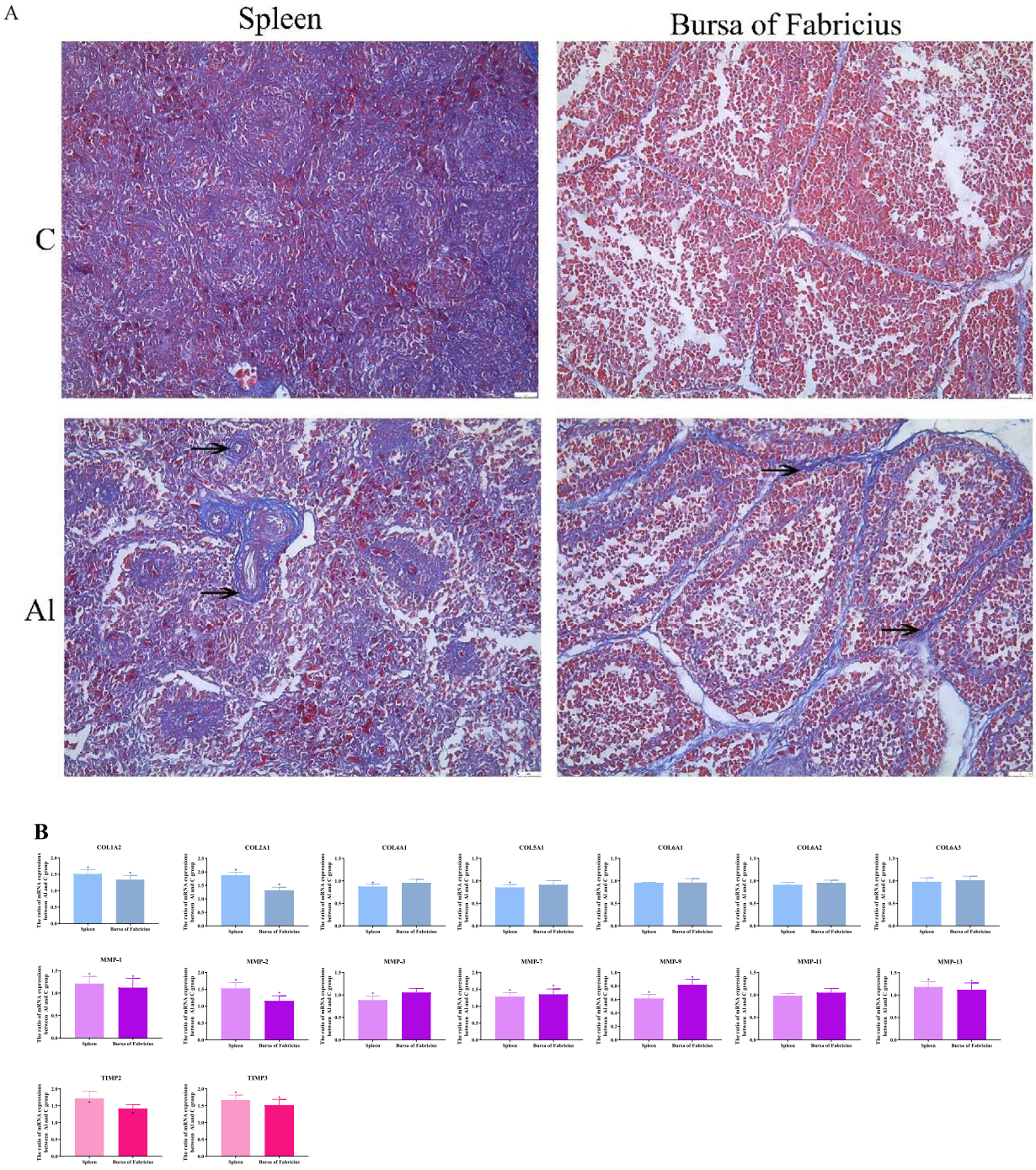

Figure 4. Al-induced fibrosis in the spleen and bursa of fabricus fibrosis of the chicks (n = 8 in each group). (A) Sections of tissue were stained with Masson trichrome staining. The arrow points indicate the accumulation of fibrin (scale bar = 20 μm); (B) effects of Al on the mRNA levels of fibrosis-related genes.

required to understand the change mechanisms and tissue specificity of NXR and CYP450 genes during acute Al poisoning.

Fibrosis is precisely regulated by the immune system for tissue repair following tissue injury. Fibrosis is caused by increased oxidative stress and may also result from an imbalance of collagen synthesis vs. degradation, which stimulates fibroblast activity (**MMPs**). NRF2 protects against pulmonary and liver fibrosis in response to oxidative stress (Cho et al., 2004). In this study, histology assays revealed an increase in collagen fibre deposition, while mRNA detection revealed abnormal expressions of fibrosis-promoting genes (MMPs and Collagens), which were potentially triggered by the excessive accumulation of oxidation indicators. Notably, the activation of profibrogenic mechanisms was more pronounced in the Al group, suggesting Al was toxic to the spleen and bursa of fabricius.

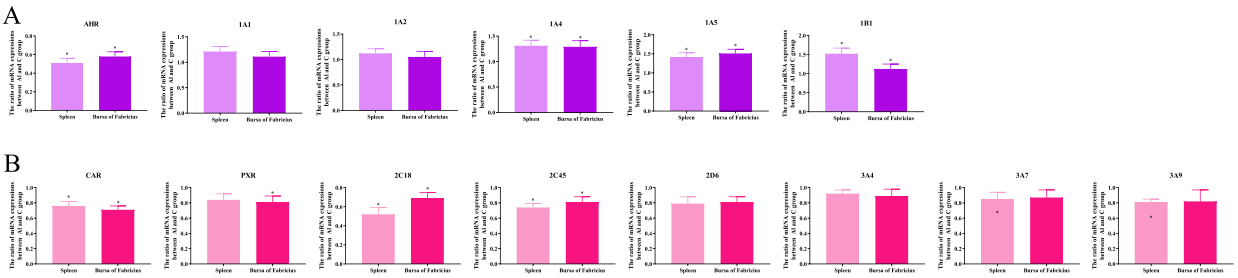

Figure 5. Bar graphs showing the effects of Al on the expression of NXRs and CYP450 genes in the spleen and bursa of fabricus. (A) The relative mRNA levels of AHR and its units; (B) the relative mRNA levels of CAR and PXR and its units.

CONCLUSIONS

Al exerts immunotoxicity effects through oxidative stress and fibrosis. The findings of this study provide a theoretical basis for the control of Al exposure and highlight the importance of further studying its mechanisms. The findings further suggest that the oxidative-redox and fibrosis related factors would be interesting novel targets for controlling acute Al immunotoxicity. Nonetheless, more studies and evaluations on the relevant biomarkers are needed to develop a more effective and accurate prediction method.

ACKNOWLEDGMENTS

This study was supported by the National Natural Science Foundation of China (No. 31902331) and the Guangdong Provincial Department of Education Featured Innovation Project (2020KTSCX133).

Compliance with ethical standards: All animal studies were approved by the institutional animal care and use committee of Foshan University.

DISCLOSURES

The authors have no conflicts of interest to report.

REFERENCES

Bao, Y., Y. Zhu, G. He, H. Ni, C. Liu, L. Ma, . . ., D. Shi. 2019. Dexmedetomidine attenuates neuroinflammation in LPS-Stimulated BV2 microglia cells through upregulation of miR-340. Drug Des Devel Ther 13:3465–3475.

Cao, Z., P. Wang, X. Gao, B. Shao, S. Zhao, and Y. Li. 2019. Lycopene attenuates aluminum-induced hippocampal lesions by inhibiting oxidative stress-mediated inflammation and apoptosis in the rat. J. Inorg. Biochem. 193:143–151.

Chen, Y. Y., and K. M. Chan. 2018. Modulations of TCDD-mediated induction of zebrafish cyp1a1 and the AHR pathway by administering Cd 2+ invivo. Chemosphere 210:577–587.

Cho, H.-Y., S. P. Reddy, M. Yamamoto, and S. R. Kleeberger. 2004. The transcription factor NRF2 protects against pulmonary fibrosis. FASEB J. 18:1258–1260.

Contini, M.d. C., N. Millen, M. González, A. Benmelej, A. Fabro, and S. Mahieu. 2016. Orchiectomy attenuates oxidative stress induced by aluminum in rats. Toxicol. Ind. Health 32:1515–1526.

Erickson, S. L., L. Alston, K. Nieves, T. K. H. Chang, S. Mani, K. L. Flannigan, and S. A. Hirota. 2019. The xenobiotic sensing pregnane X receptor regulates tissue damage and inflammation triggered by C difficile toxins. FASEB J. 34:2198–2212.

Fujii, M., M. Kishibe, M. Honma, T. Anan, and A. Ishida-Yamamoto. 2020. Aluminum chloride−induced apoptosis leads to keratinization arrest and granular parakeratosis. Am. J. Dermatopathol. 42:756–761.

Güvenç, M., M. Cellat, İ. Gökçek, G. Arkalı, A. Uyar, İ. O. Tekeli, and İ. Yavaş. 2020. Tyrosol prevents AlCl3 induced male reproductive damage by suppressing apoptosis and activating the Nrf-2/HO-1 pathway. Andrologia 52:e13499.

Gong, H., B.-k. Zhang, M. Yan, P.-f. Fang, C.-p. Hu, Y. Yang, . . ., X.-r. Fan. 2015. A protective mechanism of licorice (Glycyrrhiza uralensis): isoliquiritigenin stimulates detoxification system via Nrf2 activation. J. Ethnopharmacol. 162:134–139.

Igbokwe, I. O., E. Igwenagu, and N. A. Igbokwe. 2019. Aluminium toxicosis: a review of toxic actions and effects. Interdiscipl. Toxicol. 12:45.

Li, H., T. Huang, Y. Wang, B. Pan, L. Zhang, Q. Zhang, and Q. Niu. 2020. Toxicity of alumina nanoparticles in the immune system of mice. Nanomedicine (London, England) 15:927–946.

Liu, Q., W. Wang, Y. Zhang, Y. Cui, S. Xu, and S. Li. 2020. Bisphenol A regulates cytochrome P450 1B1 through miR-27b-3p and induces carp lymphocyte oxidative stress leading to apoptosis. Fish Shellfish Immunol 102:489–498.

Park, H.-J., M.-J. Kim, C. Rothenberger, A. Kumar, E. M. Sampson, D. Ding, . . ., S. Manohar. 2019. GSTA4 mediates reduction of cisplatin ototoxicity in female mice. Nat. Commun. 10:1–14.

Qin, X., L. Li, X. Nie, and Q. Niu. 2020. Effects of chronic aluminum lactate exposure on neuronal apoptosis and hippocampal synaptic plasticity in rats. Biol. Trace Elem. Res. 197:571–579.

Riihimäki, V., and A. Aitio. 2012. Occupational exposure to aluminum and its biomonitoring in perspective. Crit. Rev. Toxicol. 42:827–853.

Tarantino, G., S. Savastano, D. Capone, and A. Colao. 2011. Spleen: a new role for an old player? World J. Gastroenterol. 17:3776.

Wang, R., L. Wang, J. He, S. Li, X. Yang, P. Sun, . . ., H. Li. 2019. Specific inhibition of CYP4A alleviates myocardial oxidative stress and apoptosis induced by advanced glycation end-products. Front. Pharmacol. 10:876.

Willhite, C. C., G. L. Ball, and C. J. McLellan. 2012. Total allowable concentrations of monomeric inorganic aluminum and hydrated aluminum silicates in drinking water. Crit. Rev. Toxicol. 42:358–442.

Zali, H., and T. M. RezaeI. 2014. Meningioma protein-protein interaction network. Archives of Iranian medicine 17:262–272.

Zhang, Q., C. Zhang, J. Ge, M.-W. Lv, M. Talukder, K. Guo, . . ., J.-L. Li. 2020. Ameliorative effects of resveratrol against cadmium-induced nephrotoxicity via modulating nuclear xenobiotic receptor response and PINK1/Parkin-mediated Mitophagy. Food Function 11:1856–1868.